circDym prevents chronic neuropathic pain by competitive inhibition of Nlgn2 mRNA transport in neurites

Linbang Wang
The First Affiliated Hospital of Chongqing Medical University
Jingkun Liu
Xi'an Jiaotong University School of Medicine
Jiaojiao Tai
Xi'an Jiaotong University School of Medicine
Bing Wang
Xian Jiaotong University: Xi'an Jiaotong University
Shuqi Wang
University of Liverpool
Bin He
The First Affiliated Hospital of Chongqing Medical University
Zhengxue Quan (quanzx18@126.com)
The First Affiliated Hospital of Chongqing Medical University Department of Neurology
https://orcid.org/0000-0003-1778-932X

Research Article

Keywords: circDym, Neuropathic pain, synaptosome, RNA-binding protein

Posted Date: March 9th, 2021

DOI: https://doi.org/10.21203/rs.3.rs-288523/v1

Abstract

Aims: Neuropathic pain (NP) is a chronic syndrome that is refractory to current analgesics through unknown mechanisms. Epigenetic regulation in spinal dorsal horn neurons is reported to contribute to the initiation and maintenance of NP. Circular RNAs (circRNAs) are involved in various biological processes in neurons, but molecular mechanism of how the involvement in NP are lacking.

Methods: To study NP, we used a sciatic chronic constriction injury (CCI) model in C57 mice, with the level of mechanical allodynia determined using von Frey monofilaments. The injured ipsilateral spinal dorsal horns in lumbar segments (L3–L5) were collected and total RNA and protein extracted. Transcriptome sequencing, qRT-PCR, western blot analysis, and immunoprecipitation were performed. Bioinformatic analysis was conducted using R packages. The patient cohort was analysed using logistic regression analysis.

Results: circDym was identified as one of the NP-related circRNA candidates and qRT-PCR showed that its expression was significantly lower in both the CCI mouse models and in the peripheral blood of patients with NP. Overexpression of circDym significantly attenuated injury induced by NP. Further examination indicated that circDym functions by inhibiting synaptic localization of Nlgn2 mRNA by competitively binding with the RNA-binding protein, Fmrp, resulting in decreased expression of GABAAR, thus leading to the inhibition of chronic pain. Single-cell sequencing results showed that Prodynorphin-positive and Cholecystokinin-positive neurons were likely responsible for this process.

Conclusions: We identified circDym, which works through a coupling mechanism, as a novel biomarker and therapeutic target for NP.

Introduction

Neuropathic pain (NP) is a common chronic pain condition caused by traumatic damage or lesions [1]. It remains a crucial problem mainly due to a lack of understanding of the pathogenesis and molecular targets, which are known to involve multiple ion channels and their epigenetic regulation [2].

During the classical process of eukaryotic transcription, precursor mRNAs are spliced to form mature mRNAs. circRNAs are a group of non-coding RNAs that are produced by higher eukaryotes through noncanonical mRNA splicing events [3]. They primarily perform biological functions by sequestering molecules to interfere with the activities of microRNAs, proteins, and mRNAs [4]. circRNAs are recognised by their characteristic covalently closed- loop tertiary structure, which provides a longer half-life [5]. Recent evidence indicates that the expression of circRNAs is dynamic and exhibits a specific spatial and temporal profile in nervous tissues. circRNAs are more enriched than their host gene mRNA isoforms in the neuropil [6], and they have potential roles in responding to and regulating synaptic function [7]. The expression of circRNAs is dramatically downregulated following nervous system injury [8–11], while the physiological function and molecular mechanism of these changes remain unclear.

Here, we describe the molecular consequences of altered circRNA expression and continue to search for the synaptic enrichment role of circDym in NP. By conducting in vivo and in vitro experiments, we found that circDym is involved in the fragile X mental retardation protein (Fmrp)-conducted neurite transport of Nlgn2 mRNA, which is downregulated in patients with NP.

Methods And Materials

Animals

C57BL/6J mice (male, 25.0–30.0 g, 6–8 weeks old) were purchased from the Experimental Animal Centre of Chongqing Medical University (Chongqing, China) and randomly assigned to each experimental groups. Animal experimental protocols were approved by the Ethics Committee of Chongqing Medical University. Precautions were taken to minimise animal suffering and the number of animals used was kept to a minimum. All mice were housed under alternating 12-h light/dark cycles with constant temperature and humidity. Mice were given free access to food and water.

Surgery

The experiments were conducted in 8-week-old male C57BL/6 mice weighing approximately 25.0–30.0 g at study initiation. The study was approved by the Ethics Committee of the First Affiliated Hospital of Chongqing Medical University (approval number: 2020–127) and performed in accordance with the guidelines from the European Parliament and the International Association for the Study of Pain. The sciatic nerve injury model was constructed as described previously [12,13]. In brief, mice were anaesthetised with 1.5% isoflurane. The left common sciatic nerve was exposed by isolating it from the surrounding connective tissue and then crushed for 7 seconds using smooth forceps. Mice in the sham surgery group underwent the same procedure while the nerve remained intact.

Tactile allodynia evaluation

Paw mechanical withdrawal thresholds were evaluated using von Frey filaments in mice. The experimental mice were placed in a plexiglass cage with a grid at the bottom and adapted for 20 min until exploratory activities of the mice disappeared. The feet of mice were stimulated using a series of standardised von Frey filaments (0.4, 0.6, 1.4, 2.0, 4.0, 6.0, 8.0, and 15.0 g) according to the up-down method introduced by Chaplan et al. [14]. The starting filament was set to 0.6 g and the mouse withdrawal or licking reaction was observed. Fibres were applied to the paw five times and the response ratio score was calculated as described previously [15]. To avoid animal tolerance or hyperalgesia caused by frequent or prolonged stimulation, the stimulation time for each filament was limited to 1–2 seconds, and the interval between the two stimulations was 10 min.

Intrathecal (IT) injection of adeno-associated virus

All mice were weighed and randomly assigned to three groups: CircControl + control (n = 5); CircControl + chronic constriction injury (CCI)(n = 11); or circDym + CCI (n = 5). IT injections of 1×10^{12} vg /ml AAV9-shRNA-cZFP609 (adeno-associated virus-9 short-hairpin RNA; shcZFP609, HANBIO) or AAV9-shRNA-NC (shNC, HANBIO) were administered as previously described [16]. For IT injections, animals were shaved, sterilised, and gripped at the pelvic girdle. A UMP3 micropump (80330, Sigma) with a 33 gauge 45° bevelled point needle (7803-05, Hamilton) was inserted at the marked mid-spinal line. After entering the lumbar cisterna, which was indicated by a sudden tail flick, 20 μl of AAV combined with 1% lidocaine hydrochloride were delivered to each mouse. Injections were conducted at a constant injection speed, with transient mouse limb weakness signifying a successful injection [17]. The experimental group was further divided into two subgroups according to the time of injection. A one-time injection was performed in the low dose group with 20 μl AAV 21 days before surgery and a high dose group was injected two times at both 21 and 14 days before surgery.

Mouse spinal dorsal horn tissue isolation

Mice were deeply anaesthetised using isoflurane and rapidly decapitated. The lumbar enlargement segments of the spinal cords were transversely sectioned and dissected along the midline, and the dorsal part of the lumbar enlargement of sham surgery and CCI mice was collected and frozen at -80°C for subsequent processing.

Synaptosome preparation

Synaptosomes were prepared according to the detailed protocol of Dunkley et al. [18]. In brief, spinal dorsal horns were homogenised in a modulated buffer by at least 10 strokes using a Teflon-glass grinder. The homogenate was centrifuged at 1000g for 10 min, the supernatant was isolated and applied onto a discontinuous Percoll gradient from 0% to 23%, and finally centrifuged again at 31,000g for 5 min to isolate the synaptosome fraction [18].

Cell culture and differentiation

Neuro-2a cells (N2a cells, mouse origin) obtained from American Type Culture Collection were cultured in dulbecco's modified eagle medium (Invitrogen Corporation) and 10% FBS (Wisent Canadian Laboratories) as previously described [19]. During cell differentiation, the medium was switched to dulbecco's modified eagle medium with 0.5% FBS and 1 mM dbcAMP (Sigma) for 72 h [19]. The cultures were then used for qRT-PCR and fluorescence in situ hybridization (FISH) analyses.

Patients

All procedures were approved by the ethics committee of Chongqing Medical University and written informed consent was obtained from all patients. The diagnosis of chronic NP was based on clinical symptoms, signs, and characteristic findings in the electrophysiological examinations of nerve conduction functions in nerves of all limbs. Patients with autoimmune, inflammatory, psychiatric, or

neoplastic diseases were excluded. Nineteen patients with chronic NP symptoms were prospectively studied in the orthopaedics department at the First Affiliated Hospital of Chongqing Medical University, and the control group consisted of patients who lacked painful pathologies (n = 23). The Douleur Neuropathique 4 (DN4) questionnaire was used to assess the NP condition [20], which includes pain features and the occurrence of allodynia and hypoesthesia. During patient hospitalisation, 10 ml of peripheral venous blood was collected in an EDTA tube from the antecubital vein before treatment and the blood was centrifuged at 3000g for 5 min to separate the plasma. Plasma was recentrifuged for another 10 min at 1500g and stored at -80°C.

RNA isolation

Total RNA extraction from cell lines, frozen neurological tissue, and synaptosomes was performed as previously described [21]. Slight modifications were made according to the method described by Chen et al. [22]. The concentration and purity of RNA were assessed using an SMA4000 microspectrophotometer (Merinton Instrument, Inc.) and a DYY-6C electrophoresis apparatus (Liuyi. Beijing).

Reverse transcription and qRT-PCR

RNA from cell lines and tissues was reverse-transcribed using a cDNA synthesis kit (RR047A, TaKaRa, China). CEP55, MTFR2, and PIMREG RNA levels were determined by quantitative PCR using a 2X SG Fast qPCR Master Mix (High Rox, B639273, BBI) and a fluorescence quantitative PCR instrument (ABI, Foster, CA, USA). GAPDH was used as an internal control gene and all primer sequences are listed below.

circDym (mouse) F: 5'-ctgatactccactcttttct-3'

circDym (mouse) R: 5'-GACCTTAGTTAGCGCAGCAA-3'

circDYM (human) F: 5'-TGGAAGAATTGCTGTGCTGTT-3'

circDYM (human) R: 5'-TGCACCAAGATTTCCTGTTCG-3'

Gapdh (mouse) F: 5'-TGACCTCAACTACATGGTCTACA-3'

Gapdh (mouse) R: 5'-CAAATCCGTTCACACCGACCT-3'

GAPDH (human) F: 5'-ACCATCTTCCAGGAGCGAGAT-3'

GAPDH (human) R: 5'-GGGCAGAGATGATGACCCTTT-3'

Nlgn2 (mouse) F: 5'-CTGCCCTACGTCTTTGGTGT-3'

Nlgn2 (mouse) R: 5'-AGCTCTGTGTGCAGGTTGTG-3'

Sequencing and bioinformatic analysis

The illumina Truseq RNA Sample Prep Kit (illumina, San Diego, USA) was used for library construction [22] and cDNA quantification was performed using TBS380 Picogreen (Invitrogen; Waltham, USA). Low Range Ultra Agarose (Bio-Rad Laboratories Hercules, USA), cBot TruseqPE Cluster Kit (llumina, San Diego, USA), and Hiseq 2000 Truseq SBS Kit (illumina, San Diego, USA) were used for library collection, amplification, and sequencing, respectively. The quality of raw data was assessed in an orderly manner using FastQC (version 0.11.4), Cutadapt (version 1.16), and HIST2 (version 2.1.0, with parameters set to -p 10 and RNA-strandness RF).

Differentially expressed circRNAs in the spinal dorsal horn (SDH) after injury were identified by Cao et al. [13] and synaptosome-specific expression of circRNAs were obtained from Agnieszka Rybak-Wolf et al. [23]. circRNAs that are expressed at high levels in the mammalian brain were identified through GSE accession number GSE65926, while a synaptosome-specific expression set of circRNAs was downloaded from the Gene Expression Omnibus (GEO) database (GSE61991). The synaptosome-specific mRNA gene set was downloaded from the GEO database (GSE62573), while spatial single-cell transcriptome data were obtained from the Gene Expression Omnibus database (GSE103840).

StringTie (version 1.3.3b) and edgeR (version 3.24) were used to assess mRNA expression levels and differentially expressed gene (DEG) filtering. Next, DEGs were clustered and annotated with plot_cluster_exp (version 1.1.0) and GO_anot_exp (version 1.4.0).

The StarBase circinteractome was used as a screening target. The secondary and tertiary structures of circDym were formed by RNAfold (http://rna.tbi.univie.ac.at/cgi-bin/RNAWebSuite/RNAfold.cgi) and RNAComposer (http://rnacomposer.ibch.poznan.pl/). The crystal structure of Fmrp (binding site complex, PDB ID: 4OVA) was obtained from the Protein Data Bank and the nucleic acid-protein structures were predicted, scored, and visualised using NPDock (http://genesilico.pl/NPDock/help), which was performed using a hybrid docking algorithm by applying RNA-protein benchmarks. We also used catRAPID and PASSION to confirm our results (https://flagship.erc.monash.edu/PASSION/).

The Seurat package was used for integrated data analysis[24] of single-cell seq data, principal components were filtered with $P < 0.05$, and cell subclusters were identified and visualised using t-distributed stochastic neighbour embedding with resolution = 0.50 [24]. DEGs among cell subclusters were selected with a log2 fold change (FC) > 1.

Fluorescence in situ hybridization

The cells were incubated using the circDym FISH Probe (Red) and synthesised by Ribobio (Guangzhou, China). Hybridisation was performed at 55°C for 1.5 h using fluorescence-labelled probes in hybridisation buffer. After stringent washing with SSC buffer, the cell nuclei were counterstained with DAPI (Invitrogen) and images were acquired using a confocal laser-scanning microscope (Leica DM2500).

RNA immunoprecipitation (RIP)assay

The Magna RIP Kit (17–700, Millipore) was used to perform the RIP procedure. Tissues were lysed in RIP lysis buffer and immunoprecipitated with Fmrp antibody using protein magnetic beads. Next, complexes bound to the magnetic beads were immobilised by magnets, while the unbound materials were washed off. The remaining RNA was extracted.

Western blot analysis

The tissues were lysed with RIPA buffer containing protease inhibitors (Sigma-Aldrich). A BCA protein assay kit (Promega) was used for protein quantification. Western blot analysis was performed as described previously [25]. The primary antibodies used in the western blot analysis were as follows: human/mouse anti-neuroligin 2 (PA5-18668, ThermoFisher Scientific, 1:500), mouse anti-GABAARγ2 (MABN875, Millipore, 1:200), human/mouse anti-Fmrp (4317S, Cell Signaling Technology, 1:1000). Horseradish peroxidase-conjugated (HRP) goat anti-rabbit IgG (H+L) (4050–05, SouthernBiotech, 1:20000) was used as a secondary antibody. Protein levels were normalised to those of GAPDH.

Statistics

Statistical analyses were performed using GraphPad Prism 8.0 and SPSS 21.0. Two groups were analysed using t-tests and differences among groups were compared by one-way analysis of variance. $P < 0.05$ was considered significant for all statistical comparisons.

Results

circRNA expression profiles in the spinal dorsal horn of CCI and normal mice

The study design is shown in Figure 1. Our first goal was to identify potential circRNAs involved in NP. Previous microarray work has identified circRNA candidates that are potentially involved in the chronic injury of the sciatic nerve [13]. Synaptosome-enriched circRNA has also been screened by transcriptome sequencing [23] to reveal four circRNAs at the intersection of three gene sets (Figure 2A). These include two circRNAs that are upregulated (circPpp3ca, circWdr33) and two that are down-regulated (circSetbp1 and circDym). To validate our prediction that circRNAs are involved in NP, we conducted qRT-PCR of the differentially expressed circRNAs in the SDH from CCI group mice 7 and 21 days after nervous injury (NI) and compared these to the sham surgery group. As expected, mice in the sham group showed responses to mechanical stimuli in the normal range (Figure 2B). circDym was discovered as the only circRNA with a significantly different expression between the two groups (Figure 2D, E). Next, we detected a highly conserved characteristic of circDym using UCSC Genome Brower (http://genome.ucsc.edu/) (Figure 2G top), and electrophoresis and sanger sequencing confirmed the circular structure and showed the cyclization site of circDym (Figure 2G bottom). We then determined that circDym expression in the SDH after NI was positively correlated with mechanical sensitivity thresholds (Figure 2F). CircDym is likely to be involved in the regulation of synaptic pathophysiological processes. In order to confirm the synaptic location of circDym, we conducted FISH in both undifferentiated (Figure 2H, top) and differentiated (Figure 2H, bottom) N2a cells with overexpressed circDym. FISH images revealed circDym localization in

the cytoplasm, neurite, and cell nucleus of N2a cells (Figure 2H). Finally, we assessed the expression pattern of circDym in the synaptosome and soma at various post-injury times from 3–21 days. When chronic pain was initiated [26], circDym gradually decreased in both the synaptosome (Figure 2C) and soma components of the nervous tissue.

Overexpression of circDym ameliorated NP

To determine the functional role of circDym in pain development, we assessed the effects of circDym modulation on pain sensitivity in vivo. NI mice received one or two IT injections of AAV at the time of NI or sham interventions 21 days or both 21days and 14 days days before surgery. Responses to mechanical stimuli were monitored at different time points for two months (Figure 3A). A higher dose, in which mice received two IT injections of AAV, induced a stronger effect for the entire follow-up period compared with a lower, one injection dose. The second AAV injection significantly delayed the initiation time of mechanical allodynia after NI from day 13 to day 30 (Figure 3B). The circDym-overexpressing mice also avoided cold allodynia [27] and thermal hyperalgesia [28] on day 10 (Figure 3C).

circDym interacted specifically with Fmrp

In order to further determine a molecular mechanism of circDym in chronic pain formation, we conducted transcriptome sequencing in mice overexpressing circDym. The functional enrichment of DEGs was conducted and DEGs were crosschecked with synapse-enriched genes as detected by Mircsof et al. [29]. Potential targets included Rplp2, Mboat7, Casp6, and Nlgn2 (Figure 3D), and functions, including sensory system development and extracellular structure organization, were annotated (Figure 3E-G).

Recent studies have indicated important roles for circRNA and mRNA binding protein (RBP) interactions in diverse biological processes. Three RBPs with more than two potential binding sites matching to circDym and Nlgn2 mRNA were identified by StarBase and circinteractome. These included Fmrp, Eif4a3, and HuR (ELAV-like RNA binding protein 1), with Fmrp having the maximum number of binding sites (Figure 4A). Results from catRAPID and PASSION also showed perfect docking (Figure 4B, C). A previous study by Chmielewska et al. [30] also confirmed this result and proved that Fmrp binds to and conducts the axon transport of Nlgn2 mRNA in sensory neurons. Finally, the RBP RIP assay in nervous tissue confirmed that circDym bound to Fmrp (Figure 4D).

circDym repressed the role of Nlgn2 in the regulation of GABAergic synaptic protein

To explore whether circDym regulates Nlgn2 and its downstream targets, we performed an in vivo experiment. First, overexpression of circDym successfully reversed the effects of injury-induced high expression of Nlgn2 at the protein level (Figure 4E). Nlgn2 has been previously shown to play a crucial role in GABAergic synapses by regulating the expression of the GABAARγ2 subunit. Thus, we determined GABAARγ2 levels in the different groups and as predicted, the expression of GABAARγ2 protein was also upregulated in the circDym overexpression group (Figure 4F).

Nlgn2 positive neurons identified by scRNA-seq

In order to further detect the phenotype of the sensory neuron that responds to the Nlgn2-induced expression changes of GABAARγ2, we took advantage of scRNA-seq data of the spinal dorsal horn to identify their speculative regulatory mechanism. First, the scRNA-seq data were subjected to a quality control process (Figure 5A, B). Thirty-one subclusters of sensory neurons were identified using t-SNE (Figure 5C). The feature plots were utilised to display the cell-level distribution and mRNA expression of Nlgn2 and Fmrp, among them, Fmrp showed high expression in all neuron clusters. However, Nlgn2 showed higher expression in GABA positive neurons as predicted (Figure 6A), especially in Prodynorphin-positive (PDYN+) and Cholecystokinin-positive (CCK+) GABA neurons (cluster 2, 5, 8, Figure 6B)[31]. We further conducted functional analysis with these gene clusters and identified which pathways involved in “regulation of presynapse assembly”, “neuropeptide hormone activity”, and “GABA receptor activity” were activated (Figure 6C, D). Genes including SLC17A6, ADCYAP1, ADORA1, SNCA, and NPAS4, for example, are likely to be crucial in these neurons (Figure 6E).

Expression and prognosis prediction value of circDym in patients

Nineteen patients with NP (DN4 score ≥ 4) were assessed and 23 patients with no evidence of NP served as controls. Circulating circDym levels and clinical parameters were used to estimate the possibility of NP occurrence by taking advantage of logistic regression analysis (Figure 7A). Patients with NP presented with significantly lower plasma circDym levels than that in patients without pain ($P < 0.001$). In addition, diabetes mellitus and ischemia also acted as significant positive predictors of NP occurrence (Figure 7B). The quality of the model was assessed by computing the receiver operator characteristic curve (91.3%, Figure 7C).

Discussion

In this study, we used next-generation sequencing data to identify potentially relevant circRNAs involved in NP. Our results showed a relationship between circDym and allodynia development. NP was associated with a decrease in circDym in the SDH after injury. IT injection of circDym AAV prevented the development of NP in NI mice in a dose-dependent manner. The one-time injection (lower dose) delayed allodynia development for 7 days, and the two-time injections (higher dose) prevented the onset of allodynia throughout the 60 day follow-up period. Time-course experiments showed that when mice were treated early, they recovered normal mechanical sensitivity faster than that in late-treated mice, and they maintained pain relief for the experiment duration. This suggests that circDym AAV exerted long-lasting pain relief when administered in the early stages of allodynia. If the follow-up period was longer, it is possible that the neuropathic condition would not reoccur. This would be particularly relevant for patients since neurological pain is often neglected initially, causing a significant delay in treatment [32]. Based on our results, we propose that injury-related decreases in circDym expression are one of the causes of chronic pain initiation.

It has been shown that circRNAs can competitively bind to microRNAs and RBPs, serving as RBP sponges and transporters for specific molecules [33]. circRNAs have also been shown to be transported in

exosomes by RBPs towards multivesicular bodies [34]. Related to our main objective, circDym, a conserved circRNA isoform derived from Dym, has been discovered to function as a microRNA sponge by binding to miR-9 and miR-346 and regulates protein synthesis [35]. Here, we investigated whether circDym specifically inhibits the synaptic location of mRNA by competitively binding to the RNA-transporting protein.

Through in vivo and in vitro systems, the regulatory role of circDym in pain following trauma was investigated. FISH confirmed that circDym is expressed in the synaptosome. Next, we located the target by overexpressing circDym, performing RNA-seq, and searching for genes expressed in the synaptosome, followed by qRT-PCR validation. Nlgn2 was identified as a potential target gene. Neuroligin 2 (Nlgn2) is a synaptic adhesion protein that mainly participates in the maturation of inhibitory synapses and mechanical hypersensitivity [36]. The expression of Nlgn2 is upregulated in the SDH during the maintenance stage of hyperalgesic priming, leading to alterations in GABAergic function [36]. Previous studies have shown that Fmrp binds to Nlgn2 and induces synaptic transport in neurons [37]. FMRP, also known as syndromic autism protein, is an mRNA-binding protein that conducts microtubule-based mRNA transport in neurites of neurons and controls the transport and localisation of mRNAs from the cytoplasm to synaptosome [38]. Herein, we used multiple computational approaches to detect whether circDym could interact with Fmrp, and the results showed that Fmrp was ranked highly compared with other RNA-binding proteins. The binding of circDym with Fmrp was further confirmed by identifying three potential binding sites, including a shared binding site with Nlgn2 mRNA with free energy lower than − 24 kcal/mol. This result was further validated by a RIP experiment. The altered expression of Nlgn2 by circDym substantially affected GABA receptor levels and altered synaptic plasticity and changes in GABAARγ2. This is the first time that circRNA was found to be negatively associated with mRNA expression in synaptosomes by competitively binding with a neurite transporting-RBP.

The somatosensory system processes various qualities of sensations, including pain, through the molecular diversity of dorsal horn sensory neurons [39]. Here, we observed that Fmrp is universally expressed and that two clusters of neurons have a relatively high expression of Nlgn2, including inhibitory PDYN + neurons and excitatory CCK + neurons. Inhibitory PDYN + neurons are located at lamina II, gated the allodynic pain pathway, and terminated the excitatory somatostatin-positive neurons that induced mechanical pain [40–42]. Excitatory CCK + neurons are a group of low-threshold processing interneurons that play a crucial role during chronic pain [43] and are activated under pathological conditions. Thus, associating Nlgn2 expression to the specific molecular types of dorsal horn neurons reveals transmitting sensory modalities and clarifies the mechanism for how the dorsal horn disrupts sensory processing and causes chronic pain.

Currently, there is a lack of objective indicators used to identify patients with NP [44]. Circulating circRNAs are emerging as non-invasive biomarkers for detecting human diseases [45]. Herein, CircDym in the plasma increased after the establishment of the neuropathic state in mice. Patients diagnosed with NP in the context of severe chronic leg ischemia exhibited elevated expression of circulating circDym in the plasma. Moreover, univariate logistic regression analyses showed that circulating circDym in plasma was

correlated with NP severity. Previous reports have shown that age, diabetes, and peripheral arterial lesions are the main risk factors for NP [46]. Taken together with circulating circDym levels through a multiple logistic regression framework, our diagnostic power is substantially improved. Thus, our results suggest that analysis of circulating circDym in pain states may provide useful information for pain assessment and management.

We believe that our in depth characterisation of these molecular events will enhance future explorations into circRNA-mediated regulation and function underlying the biology of neuroinjury and its associated disorders.

Abbreviations

NP, neuropathic pain; Fmrp, fragile X mental retardation protein; IT, Intrathecal; CCI, chronic constriction injury; FISH, fluorescence in situ hybridization; DEG, differentially expressed gene; RIP, RNA immunoprecipitation; NI, nervous injury; PDYN+, prodynorphin-positive; CCK+, Cholecystokinin-positive.

Declarations

Funding

Not applicable

Conflicts of interest

The author declares that there is no conflict of interest that could be perceived as prejudicing the impartiality of the research reported.

Availability of data and material

Not applicable

Code availability

Not applicable

Author contributions

QZX and WLB conceived of and designed the experiments. QZX provided human tissue that was analysed and diagnosed by WLB. WB performed RT-qPCR and analysed the data. WLB and LJK performed in vitro experiments. TJJ and WSQ contributed to data interpretation and manuscript preparation. All authors read, revised, and approved the final manuscript.

Ethical approval

We confirm that the journal's guidelines related to ethical publication have been carefully read, and this report is consistent with all guidelines.

Consent to participate

Not applicable

Consent for publication

Not applicable

References

1. Colloca L, Ludman T, Bouhassira D, Baron R, Dickenson AH, Yarnitsky D, Freeman R, Truini A, Attal N, Finnerup NB, Eccleston C, Kalso E, Bennett DL, Dworkin RH, Raja SN (2017) Neuropathic pain. Nature reviews Disease primers 3:17002. doi:10.1038/nrdp.2017.2
2. Finnerup NB, Kuner R, Jensen TS (2021) Neuropathic Pain: From Mechanisms to Treatment. Physiological reviews 101 (1):259-301. doi:10.1152/physrev.00045.2019
3. Chen LL (2020) The expanding regulatory mechanisms and cellular functions of circular RNAs. Nature reviews Molecular cell biology 21 (8):475-490. doi:10.1038/s41580-020-0243-y
4. Chen W, Schuman E (2016) Circular RNAs in Brain and Other Tissues: A Functional Enigma. Trends in neurosciences 39 (9):597-604. doi:10.1016/j.tins.2016.06.006
5. Wen G, Zhou T, Gu W (2020) The potential of using blood circular RNA as liquid biopsy biomarker for human diseases. Protein & cell. doi:10.1007/s13238-020-00799-3
6. You X, Vlatkovic I, Babic A, Will T, Epstein I, Tushev G, Akbalik G, Wang M, Glock C, Quedenau C, Wang X, Hou J, Liu H, Sun W, Sambandan S, Chen T, Schuman EM, Chen W (2015) Neural circular RNAs are derived from synaptic genes and regulated by development and plasticity. Nature neuroscience 18 (4):603-610. doi:10.1038/nn.3975
7. Xu K, Zhang Y, Xiong W, Zhang Z, Wang Z, Lv L, Liu C, Hu Z, Zheng YT, Lu L, Hu XT, Li J (2020) CircGRIA1 shows an age-related increase in male macaque brain and regulates synaptic plasticity and synaptogenesis. Nature communications 11 (1):3594. doi:10.1038/s41467-020-17435-7
8. Zhu H, Xing Z, Zhao Y, Hao Z, Li M (2020) The Role of Circular RNAs in Brain Injury. Neuroscience 428:50-59. doi:10.1016/j.neuroscience.2019.12.018
9. Qu X, Li Z, Chen J, Hou L (2020) The emerging roles of circular RNAs in CNS injuries. Journal of neuroscience research 98 (7):1485-1497. doi:10.1002/jnr.24591
10. Ray P, Torck A, Quigley L, Wangzhou A, Neiman M, Rao C, Lam T, Kim JY, Kim TH, Zhang MQ, Dussor G, Price TJ (2018) Comparative transcriptome profiling of the human and mouse dorsal root ganglia: an RNA-seq-based resource for pain and sensory neuroscience research. Pain 159 (7):1325-1345. doi:10.1097/j.pain.0000000000001217

11. Yuan J, Botchway BOA, Zhang Y, Wang X, Liu X (2020) Role of Circular Ribonucleic Acids in the Treatment of Traumatic Brain and Spinal Cord Injury. Molecular neurobiology 57 (10):4296-4304. doi:10.1007/s12035-020-02027-9
12. Zhou ZB, Niu YL, Huang GX, Lu JJ, Chen A, Zhu L (2018) Silencing of circRNA.2837 Plays a Protective Role in Sciatic Nerve Injury by Sponging the miR-34 Family via Regulating Neuronal Autophagy. Molecular therapy Nucleic acids 12:718-729. doi:10.1016/j.omtn.2018.07.011
13. Cao S, Deng W, Li Y, Qin B, Zhang L, Yu S, Xie P, Xiao Z, Yu T (2017) Chronic constriction injury of sciatic nerve changes circular RNA expression in rat spinal dorsal horn. Journal of pain research 10:1687-1696. doi:10.2147/jpr.s139592
14. Maess B, Schröger E, Widmann A (2016) High-pass filters and baseline correction in M/EEG analysis. Commentary on: "How inappropriate high-pass filters can produce artefacts and incorrect conclusions in ERP studies of language and cognition". Journal of neuroscience methods 266:164-165. doi:10.1016/j.jneumeth.2015.12.003
15. An G, Li W, Yan T, Li S (2014) Estrogen rapidly enhances incisional pain of ovariectomized rats primarily through the G protein-coupled estrogen receptor. International journal of molecular sciences 15 (6):10479-10491. doi:10.3390/ijms150610479
16. Li D, Liu C, Yang C, Wang D, Wu D, Qi Y, Su Q, Gao G, Xu Z, Guo Y (2017) Slow Intrathecal Injection of rAAVrh10 Enhances its Transduction of Spinal Cord and Therapeutic Efficacy in a Mutant SOD1 Model of ALS. Neuroscience 365:192-205. doi:10.1016/j.neuroscience.2017.10.001
17. Guo Y, Wang D, Qiao T, Yang C, Su Q, Gao G, Xu Z (2016) A Single Injection of Recombinant Adeno-Associated Virus into the Lumbar Cistern Delivers Transgene Expression Throughout the Whole Spinal Cord. Molecular neurobiology 53 (5):3235-3248. doi:10.1007/s12035-015-9223-1
18. Dunkley PR, Jarvie PE, Robinson PJ (2008) A rapid Percoll gradient procedure for preparation of synaptosomes. Nature protocols 3 (11):1718-1728. doi:10.1038/nprot.2008.171
19. Tremblay RG, Sikorska M, Sandhu JK, Lanthier P, Ribecco-Lutkiewicz M, Bani-Yaghoub M (2010) Differentiation of mouse Neuro 2A cells into dopamine neurons. Journal of neuroscience methods 186 (1):60-67. doi:10.1016/j.jneumeth.2009.11.004
20. Bouhassira D, Lantéri-Minet M, Attal N, Laurent B, Touboul C (2008) Prevalence of chronic pain with neuropathic characteristics in the general population. Pain 136 (3):380-387. doi:10.1016/j.pain.2007.08.013
21. Ueberham U, Lange P, Ueberham E, Brückner MK, Hartlage-Rübsamen M, Pannicke T, Rohn S, Cross M, Arendt T (2009) Smad2 isoforms are differentially expressed during mouse brain development and aging. International journal of developmental neuroscience : the official journal of the International Society for Developmental Neuroscience 27 (5):501-510. doi:10.1016/j.ijdevneu.2009.04.001
22. Chen BJ, Ueberham U, Mills JD, Kirazov L, Kirazov E, Knobloch M, Bochmann J, Jendrek R, Takenaka K, Bliim N, Arendt T, Janitz M (2017) RNA sequencing reveals pronounced changes in the noncoding

transcriptome of aging synaptosomes. Neurobiology of aging 56:67-77. doi:10.1016/j.neurobiolaging.2017.04.005

23. Rybak-Wolf A, Stottmeister C, Glažar P, Jens M, Pino N, Giusti S, Hanan M, Behm M, Bartok O, Ashwal-Fluss R, Herzog M, Schreyer L, Papavasileiou P, Ivanov A, Öhman M, Refojo D, Kadener S, Rajewsky N (2015) Circular RNAs in the Mammalian Brain Are Highly Abundant, Conserved, and Dynamically Expressed. Molecular cell 58 (5):870-885. doi:10.1016/j.molcel.2015.03.027
24. Butler A, Hoffman P, Smibert P, Papalexi E, Satija R (2018) Integrating single-cell transcriptomic data across different conditions, technologies, and species. Nature biotechnology 36 (5):411-420. doi:10.1038/nbt.4096
25. Zeng Y, Liu Y, Wu M, Liu J, Hu Q (2012) Activation of TrkB by 7,8-dihydroxyflavone prevents fear memory defects and facilitates amygdalar synaptic plasticity in aging. Journal of Alzheimer's disease : JAD 31 (4):765-778. doi:10.3233/jad-2012-120886
26. Peng J, Gu N, Zhou L, U BE, Murugan M, Gan WB, Wu LJ (2016) Microglia and monocytes synergistically promote the transition from acute to chronic pain after nerve injury. Nature communications 7:12029. doi:10.1038/ncomms12029
27. Choi Y, Yoon YW, Na HS, Kim SH, Chung JM (1994) Behavioral signs of ongoing pain and cold allodynia in a rat model of neuropathic pain. Pain 59 (3):369-376. doi:10.1016/0304-3959(94)90023-x
28. Hargreaves K, Dubner R, Brown F, Flores C, Joris J (1988) A new and sensitive method for measuring thermal nociception in cutaneous hyperalgesia. Pain 32 (1):77-88. doi:10.1016/0304-3959(88)90026-7
29. Mircsof D, Langouët M, Rio M, Moutton S, Siquier-Pernet K, Bole-Feysot C, Cagnard N, Nitschke P, Gaspar L, Žnidarič M, Alibeu O, Fritz AK, Wolfer DP, Schröter A, Bosshard G, Rudin M, Koester C, Crestani F, Seebeck P, Boddaert N, Prescott K, Hines R, Moss SJ, Fritschy JM, Munnich A, Amiel J, Brown SA, Tyagarajan SK, Colleaux L (2015) Mutations in NONO lead to syndromic intellectual disability and inhibitory synaptic defects. Nature neuroscience 18 (12):1731-1736. doi:10.1038/nn.4169
30. Chmielewska JJ, Kuzniewska B, Milek J, Urbanska K, Dziembowska M (2019) Neuroligin 1, 2, and 3 Regulation at the Synapse: FMRP-Dependent Translation and Activity-Induced Proteolytic Cleavage. Molecular neurobiology 56 (4):2741-2759. doi:10.1007/s12035-018-1243-1
31. Häring M, Zeisel A, Hochgerner H, Rinwa P, Jakobsson JET, Lönnerberg P, La Manno G, Sharma N, Borgius L, Kiehn O, Lagerström MC, Linnarsson S, Ernfors P (2018) Neuronal atlas of the dorsal horn defines its architecture and links sensory input to transcriptional cell types. Nature neuroscience 21 (6):869-880. doi:10.1038/s41593-018-0141-1
32. Castelnuovo G, Giusti EM, Manzoni GM, Saviola D, Gatti A, Gabrielli S, Lacerenza M, Pietrabissa G, Cattivelli R, Spatola CA, Corti S, Novelli M, Villa V, Cottini A, Lai C, Pagnini F, Castelli L, Tavola M, Torta R, Arreghini M, Zanini L, Brunani A, Capodaglio P, D'Aniello GE, Scarpina F, Brioschi A, Priano L, Mauro A, Riva G, Repetto C, Regalia C, Molinari E, Notaro P, Paolucci S, Sandrini G, Simpson SG, Wiederhold

B, Tamburin S (2016) Psychological Treatments and Psychotherapies in the Neurorehabilitation of Pain: Evidences and Recommendations from the Italian Consensus Conference on Pain in Neurorehabilitation. Frontiers in psychology 7:115. doi:10.3389/fpsyg.2016.00115

33. Wawrzyniak O, Zarębska Ż, Kuczyński K, Gotz-Więckowska A, Rolle K (2020) Protein-Related Circular RNAs in Human Pathologies. Cells 9 (8). doi:10.3390/cells9081841
34. Jiang B, Hildt E (2020) Intracellular Trafficking of HBV Particles. Cells 9 (9). doi:10.3390/cells9092023
35. Song R, Bai Y, Li X, Zhu J, Zhang H, Shi Y, Li K, Wang B, Zhang H, Yang Y, Zhang Z (2020) Plasma Circular RNA DYM Related to Major Depressive Disorder and Rapid Antidepressant Effect Treated by Visual Cortical Repetitive Transcranial Magnetic Stimulation. Journal of affective disorders 274:486-493. doi:10.1016/j.jad.2020.05.109
36. Kim JY, Megat S, Moy JK, Asiedu MN, Mejia GL, Vagner J, Price TJ (2016) Neuroligin 2 regulates spinal GABAergic plasticity in hyperalgesic priming, a model of the transition from acute to chronic pain. Pain 157 (6):1314-1324. doi:10.1097/j.pain.0000000000000513
37. Parente DJ, Garriga C, Baskin B, Douglas G, Cho MT, Araujo GC, Shinawi M (2017) Neuroligin 2 nonsense variant associated with anxiety, autism, intellectual disability, hyperphagia, and obesity. American journal of medical genetics Part A 173 (1):213-216. doi:10.1002/ajmg.a.37977
38. Pilaz LJ, Lennox AL, Rouanet JP, Silver DL (2016) Dynamic mRNA Transport and Local Translation in Radial Glial Progenitors of the Developing Brain. Current biology : CB 26 (24):3383-3392. doi:10.1016/j.cub.2016.10.040
39. Tsuda M (2018) Modulation of Pain and Itch by Spinal Glia. Neuroscience bulletin 34 (1):178-185. doi:10.1007/s12264-017-0129-y
40. Pan X, Wang C, Li Y, Zhu L, Zhang T (2018) RETRACTED: Protective autophagy induced by physcion suppresses hepatocellular carcinoma cell metastasis by inactivating the JAK2/STAT3 Axis. Life sciences 214:124-135. doi:10.1016/j.lfs.2018.10.064
41. Wildner H, Das Gupta R, Bröhl D, Heppenstall PA, Zeilhofer HU, Birchmeier C (2013) Genome-wide expression analysis of Ptf1a- and Ascl1-deficient mice reveals new markers for distinct dorsal horn interneuron populations contributing to nociceptive reflex plasticity. The Journal of neuroscience : the official journal of the Society for Neuroscience 33 (17):7299-7307. doi:10.1523/jneurosci.0491-13.2013
42. Shi TJ, Xiang Q, Zhang MD, Barde S, Kai-Larsen Y, Fried K, Josephson A, Glück L, Deyev SM, Zvyagin AV, Schulz S, Hökfelt T (2014) Somatostatin and its 2A receptor in dorsal root ganglia and dorsal horn of mouse and human: expression, trafficking and possible role in pain. Molecular pain 10:12. doi:10.1186/1744-8069-10-12
43. Wagner KM, Roeder Z, Desrochers K, Buhler AV, Heinricher MM, Cleary DR (2013) The dorsomedial hypothalamus mediates stress-induced hyperalgesia and is the source of the pronociceptive peptide cholecystokinin in the rostral ventromedial medulla. Neuroscience 238:29-38. doi:10.1016/j.neuroscience.2013.02.009

44. Sisignano M, Lötsch J, Parnham MJ, Geisslinger G (2019) Potential biomarkers for persistent and neuropathic pain therapy. Pharmacology & therapeutics 199:16-29. doi:10.1016/j.pharmthera.2019.02.004
45. Pardini B, Sabo AA, Birolo G, Calin GA (2019) Noncoding RNAs in Extracellular Fluids as Cancer Biomarkers: The New Frontier of Liquid Biopsies. Cancers 11 (8). doi:10.3390/cancers11081170
46. Callaghan BC, Gallagher G, Fridman V, Feldman EL (2020) Diabetic neuropathy: what does the future hold? Diabetologia 63 (5):891-897. doi:10.1007/s00125-020-05085-9

Figures

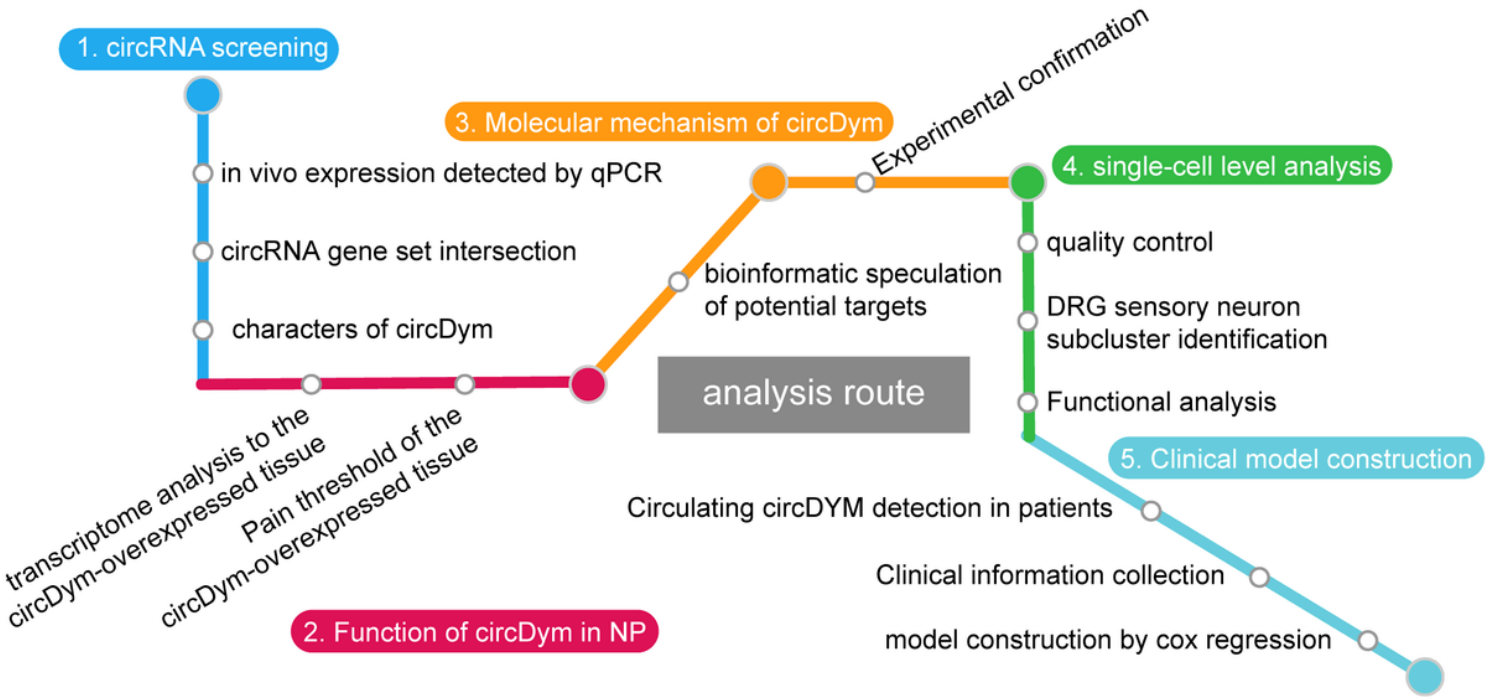

Figure 1

Flow chart of the study procedure.

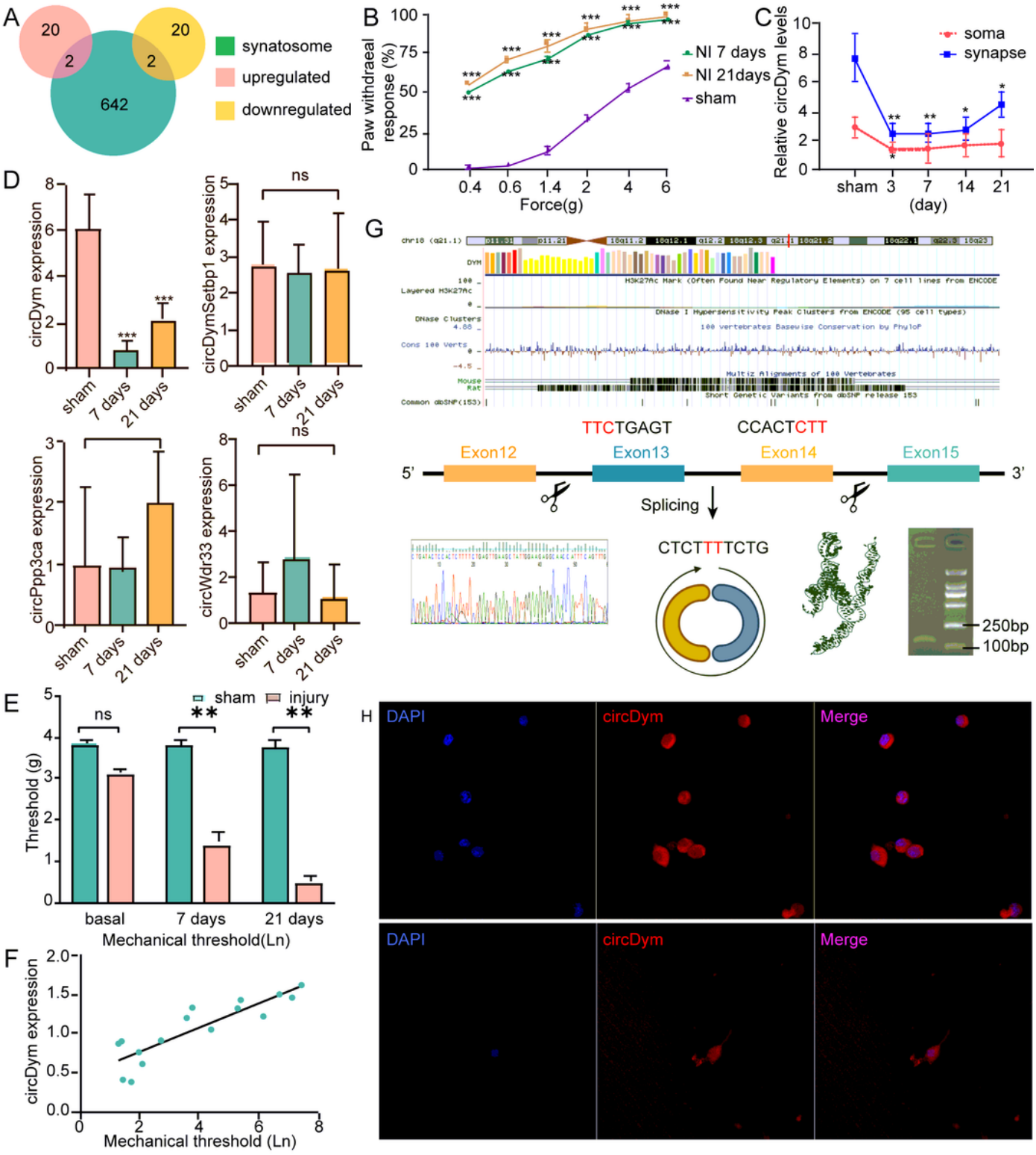

Figure 2

Identification of aberrantly expressed circRNAs in NP. (A) Intersection of NP-related circRNAs and synaptic-enriched circRNAs. (B) Nocifensive responses to mechanical stimuli in CCI (n = 5) and sham surgery mice (n = 5). (one-way repeated measures ANOVA). (C) Expression patterns over time for circDym between neuron somas and synaptosomes. (D) qPCR results show differential circRNA expression profiles in the SDH of mice in the CCI and sham surgery groups (n = 7 per group, two-way ANOVA). (E)

The mechanical threshold of CCI and sham surgery mice. (F) Correlation between allodynia severity (quantified by mechanical thresholds) and circDym expression in the spinal dorsal horn of mice (n=5) following sciatic NI. (G) The conservativeness of CircDym is shown on the top. Sanger sequencing of circDym and Agarose H gel electrophoresis was performed. The loop diagram shows the circular character of circDym. (H) circDym levels in different groups were detected by immunofluorescence assay. ***P < 0.001; **P < 0.01; *P < 0.05; ns, non-significance.

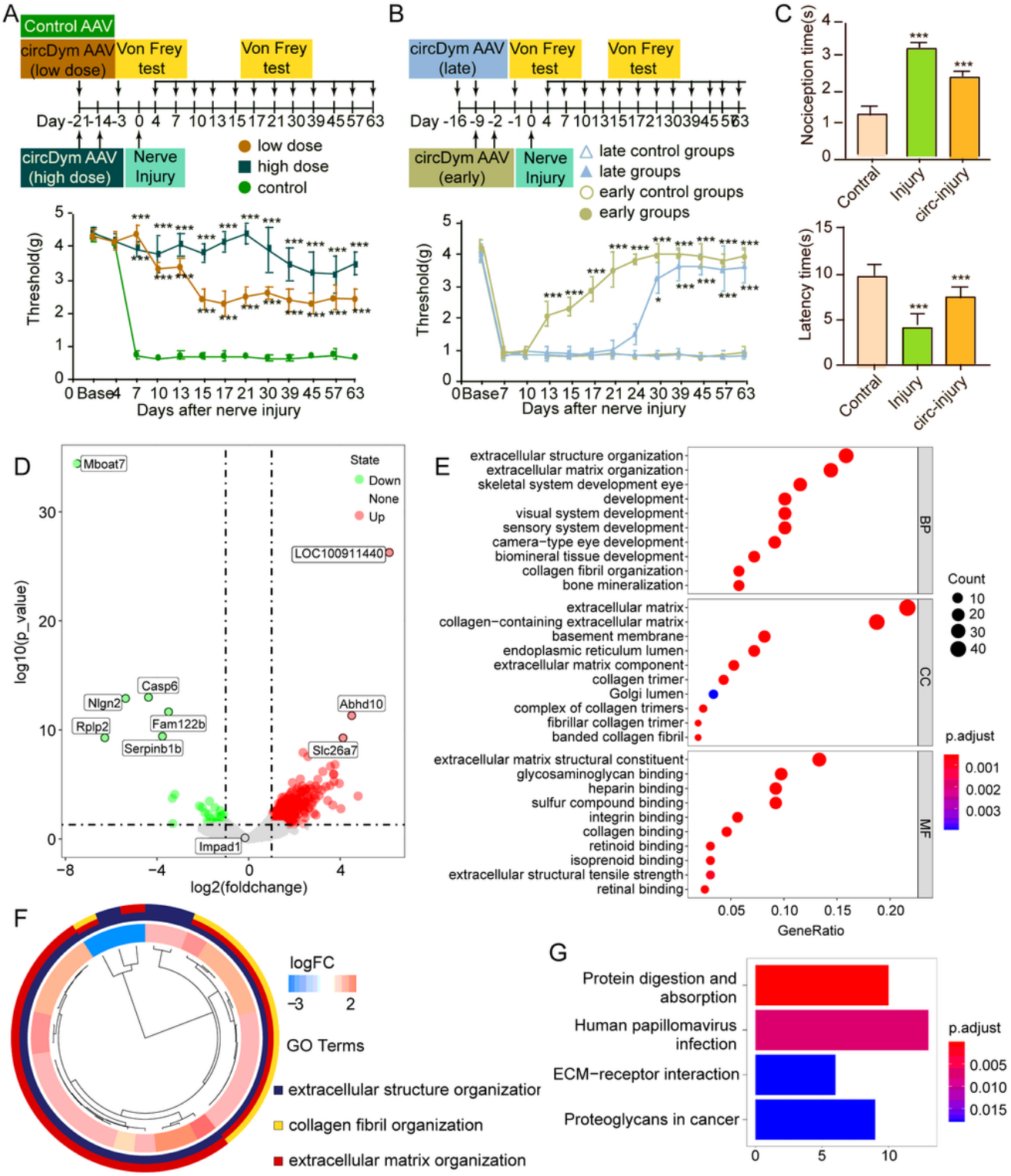

Figure 3

circDym AAV reverses NP in mice subjected to CCI. (A) Top: Intrathecal administration protocol for circDym overexpression AAV [one time (n = 5) or two times (n = 5)] or control AAV (n = 5). Bottom: The threshold force (g) required to elicit responses for the groups in a time-dependent manner. ***P < 0.001, versus control group (two-way repeated measures ANOVA). (B) Top: Intrathecal administration protocol for circDym overexpression AAV [starting early or late before CCI] or control AAV (n = 5). Bottom: Time course scale of the threshold force. ***P < 0.001, *P < 0.05, versus control group (two-way repeated measures ANOVA). (C) Thermal hyperalgesia and cold allodynia groups versus the control group are indicated in the legend. (***P < 0.001, n = 5; t-test). (D) Volcano plot showing the upregulated (in red) and downregulated (in green) mRNAs in mice with overexpressed circDym. (E-F) Gene Ontology (GO) analyses of differentially expressed mRNAs, including molecular function (MF), biological process (BP), and cellular component (CC) categories (G) KEGG analysis of differentially expressed mRNAs.

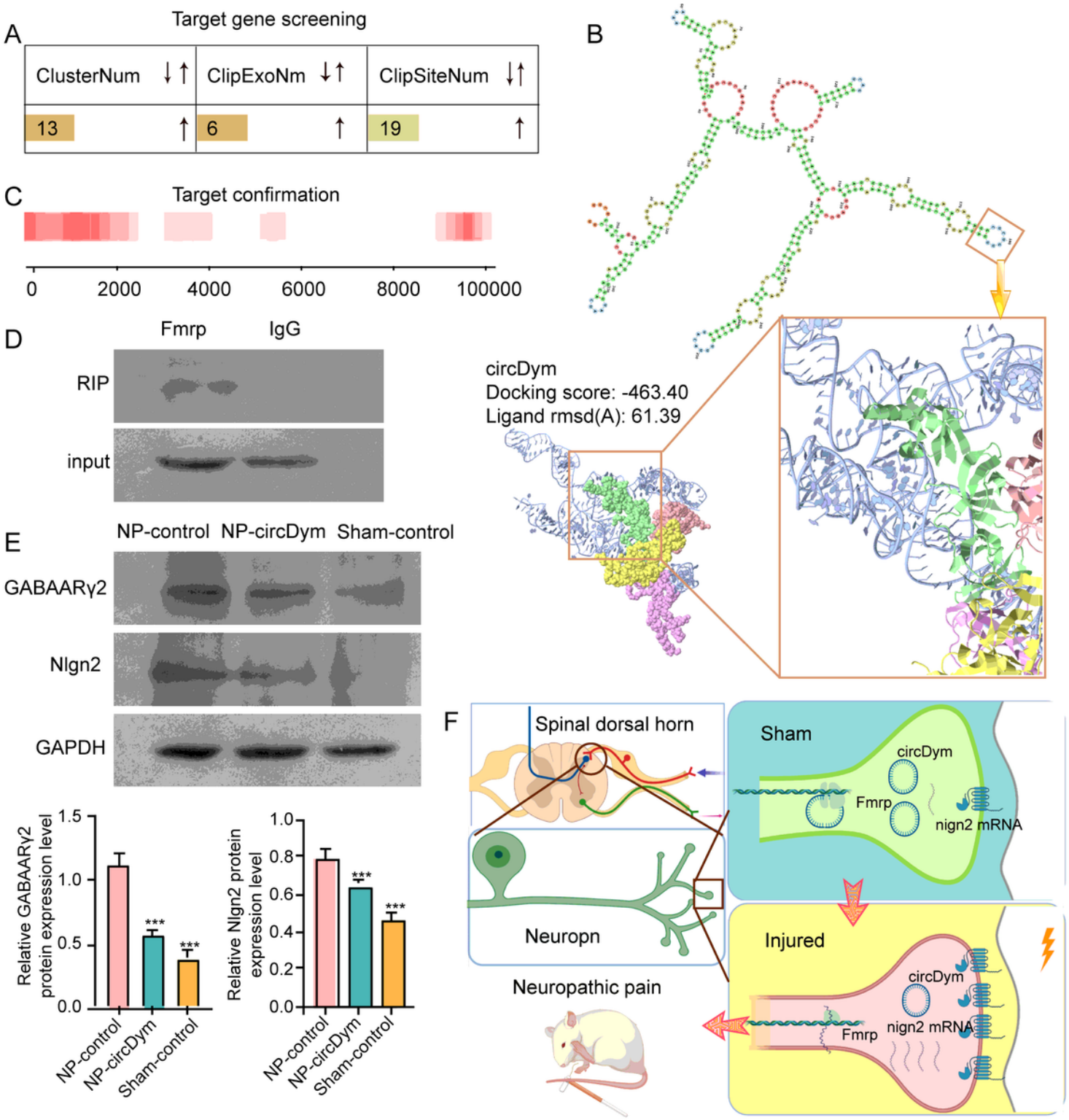

Figure 4

circDym is involved in the initiation of chronic pain by the absence of competitive binding to Fmrp. (A) The screening of potential RBPs that bind to circDym and RBP by StarBase. Fmrp was selected as a potential target. (B) The binding site of circDym was located using catRAPID. (C) HDock identifies the binding sites between circDym (blue) and Fmrp (rainbow). The secondary structure of circDym highlights the interactive sites with Fmrp (yellow box). (D) Schematic diagram of the circDym regulatory

mechanism. (E) The effects of circDym overexpression on Nlgn2 and GABAARγ2 protein levels by western blotting P < 0.05. (F) Anti-Fmrp and anti-IgG (control) immunoprecipitation and western blot.

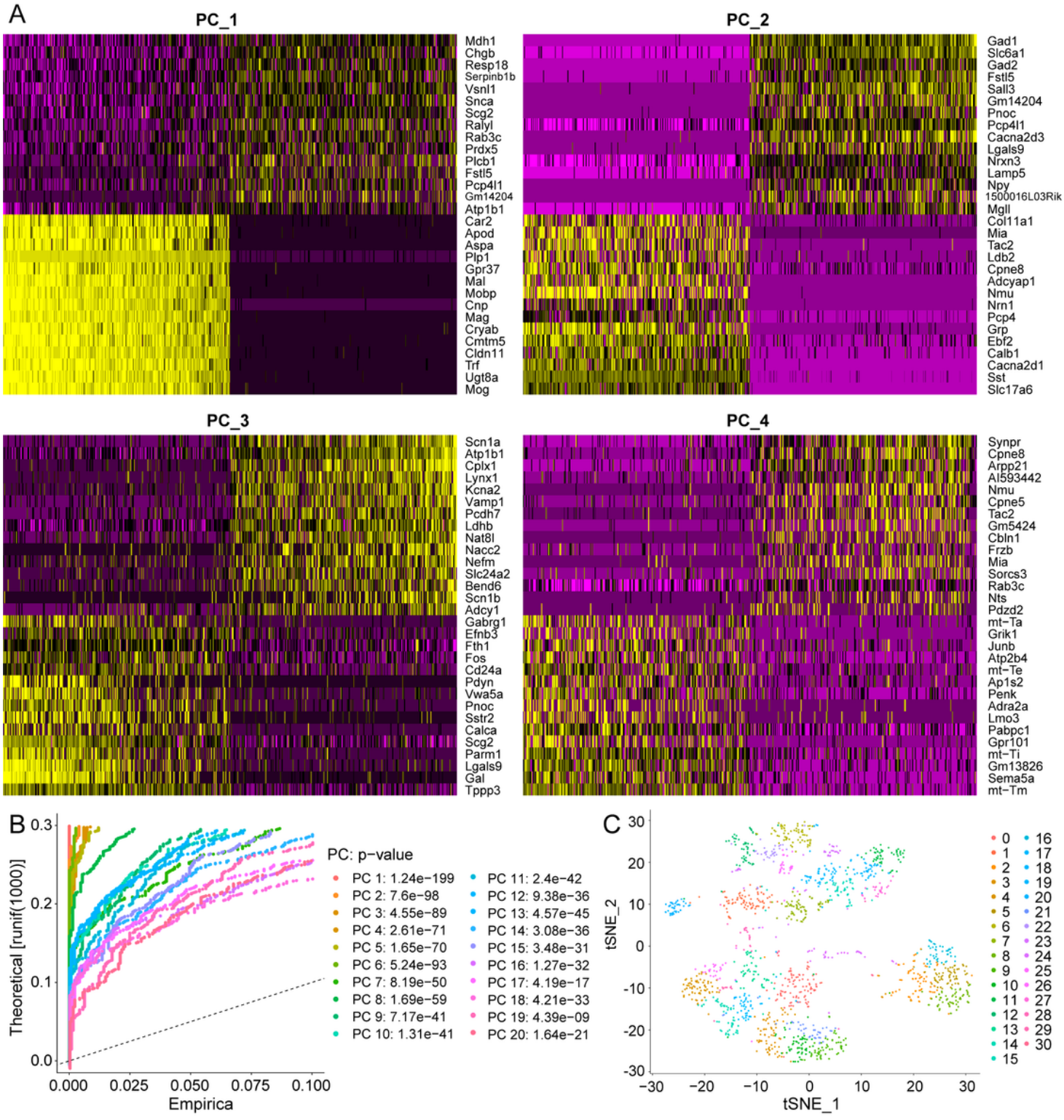

Figure 5

Single-cell RNA-seq quality control data. (A) Genes related to principal component (PC)1, PC2, PC3, and PC4. (B) Twenty principal components were identified by PCA with estimated P values < 0.05. (C) The

tSNE algorithm was used for dimensionality reduction and 30 subclusters of sensory neurons were successfully classified.

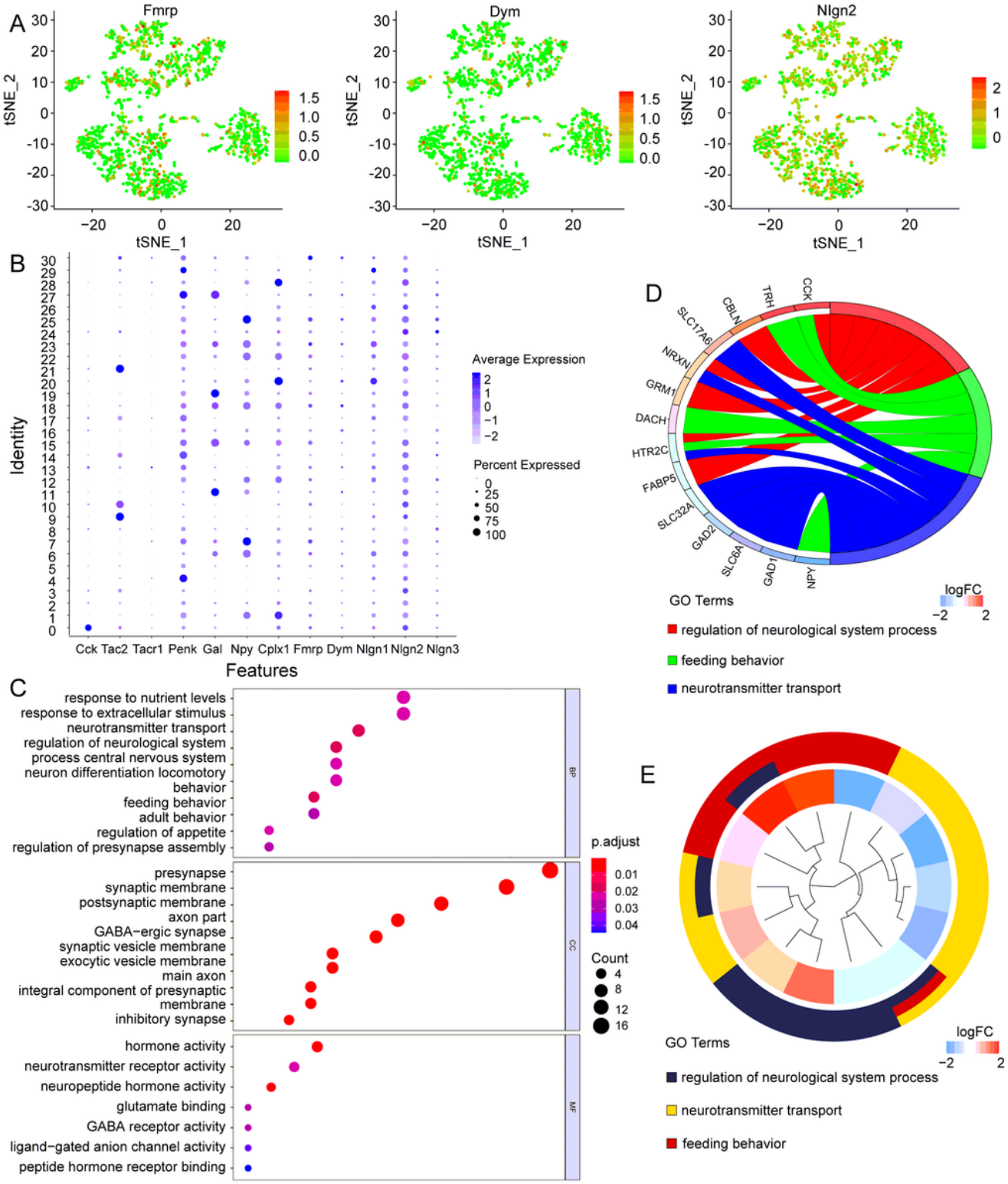

Figure 6

Identification of GABA neurons with Nlgn2 expression revealing molecular characteristics of Nlgn2+ sensory neurons and their functions based on single-cell RNA-seq data. (A) Fmrp, Dym mRNA, and Nlgn2 expression distribution after integration with Seurat canonical correlation analysis. (B) Markers of

different types of sensory neurons among the cell groups. (C) GO analysis identifies important biological functions of Nlgn2+ neurons, including three categories: biological process (BP), cellular component (CC), and molecular function (MF). (D-E) Circular dendrogram showing the hub genes and their assigned biological functions by applying Gene Ontology analysis.

A

	pain(n=19)	non-pain(n=23)
ischemia	14	9
hypertension	7	6
Diabetes mellitus	11	6
sex	9	7
BMI	26.89074168	26.02982082
+-	1.820811184	2.165295092
age	71.26315789	69.2173913
+-	3.856338293	5.071816258

B

	Coefficient	Standard error	P value
Ischemia	-1.713	0.958	0.074
circDYM	-3.909	1.254	0.002
Diabetes	-2.6	1.177	0.027
Constant	4.369	1.432	0.002

C

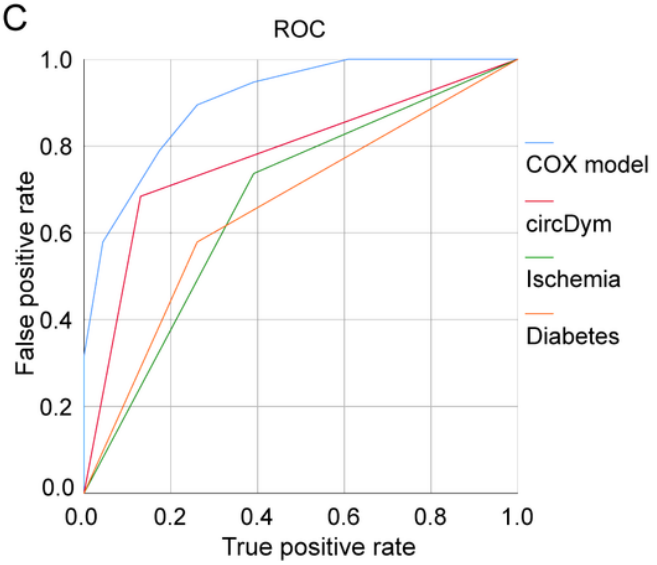

Figure 7

Multiple logistic regression model to predict the occurrence of neuropathic pain in patients. (A) Clinical characteristics of the patients. (B) Variables in the diagnostic model include circulating circDym in plasma, diabetes mellitus, and ischemia. (C) ROC curves of the models, variables were applied individually or I combination.